Biotechnology Reports 27 (2020) e00518

Contents lists available at ScienceDirect

Biotechnology Reports

journal homepage: www.elsevier.com/locate/btre

Green synthesis of copper nanoparticles using *Celastrus paniculatus* Willd. leaf extract and their photocatalytic and antifungal properties

Suresh Chand Mali, Anita Dhaka, Chanda Kumari Githala, Rohini Trivedi*

Laboratory of Plant Pathology, Department of Botany, University College of Science, Mohanlal Sukhadia University, Udaipur, 313001, Rajasthan, India

ARTICLE INFO

Article history:
Received 8 July 2020
Received in revised form 27 July 2020
Accepted 10 August 2020

Keywords:
Antifungal
Copper nanoparticles
Green synthesis
Methylene blue
Photocatalytic

ABSTRACT

This research aimed to explore the eco-friendly green synthesis of copper nanoparticles (CuNPs) using *Celastrus paniculatus* leaves extract. Primarily, the biosynthesized CuNPs characterized by UV–vis spectroscopy showed an absorption peak at 269 nm. Further, The SEM and TEM studies revealed the spherical shape of particles with size ranged between 2−10 nm with an average particle diameter of 5 nm. FT-IR analysis confirmed the presence of functional groups —OH, C=C and C—H triggers the synthesis of CuNPs. The negative zeta potential -22.2 mV indicated the stability of CuNPs was confirmed by DLS and the composition and purity by EDS studies. Further, the photocatalytic property of the CuNPs was divulged by their methylene blue dye degradation potential. The reaction kinetics followed pseudo-first-order with k-values (rate constant) 0.0172 min^{-1}. In addition, this material was found to be a good antifungal agent against plant pathogenic fungi *Fusarium oxysporum* showed 76.29 ± 1.52 maximum mycelial inhibition.

1. Introduction

Modernization and industrialization discharged a bulk amount of industrial effluents along with organic dyes into the water bodies. Organic dyes are widely used as a colorant in various industries such as textile, leather tanning, paper, cosmetics, pharmaceutical, and plastic [1]. These organic dyes highly toxic, carcinogenic, and non-degradable, can cause serious health problems such as skin diseases, cancer, allergic reactions, and mutation for people [2,3]. For such purposes, numerous water treatment approaches have been explored for the treatment of industrial wastewater effluents such as precipitation, coagulation, electrolysis, activated carbon, oxidation, and reduction reactions [4]. However, these techniques are costly and often transfer toxic pollutants to water bodies. Therefore, need to develop an eco-friendly and cost-effective method for the degradation of an organic pollutant from wastewater [5]. Recently, biosynthesized nanoparticles (NPs) attracted much attention due to their photocatalytic application in the degradation of organic dyes [6]. Different types of plants and their derived products have been used successfully in the synthesis of different green nanoparticles of zinc oxide [7,8], platinum [9], palladium [10], silver [11,12], cobalt [13], magnetic [14], and gold [15].

However, there are several studies on CuNPs synthesis using different plants extract [16–23] have been reported but the study of application of CuNPs on the treatment of dye effluent is limited. The agriculture sector exploits different kind of pesticides, herbicides, and antimicrobial [24,25] substances to control plant diseases. These substances are responsible for soil pollution as well as biomagnification in living organisms [26,27]. Despite photocatalytic activity, CuNPs attracted more attention due to its nontoxic, antimicrobial efficacy in controlling plant diseases. An extensive literature survey revealed that the antifungal activity of CuNPs mostly tested against human pathogenic fungi [28]. The least study conducted on CuNPs antifungal activity on plant pathogenic fungi, so, there is a crucial need for more assessment and evaluation in this field [29].

Nowadays nanomaterials are of huge interest due to a wide range of applications in chemical, biological, and environmental sciences [30,31]. The NPs exhibited a variety of applications, including optical, electrical, thermal conductivity, catalysts, antioxidant, antimicrobial, and anticancer activity. Among the NPs, CuNPs have great attention due to its catalytic, high electrical conductivity, optical, antifungal, and antibacterial properties [6,32–34]. The unique physical and chemical properties of NPs which are not exhibited by the bulk materials, received much attention to synthesis of NPs. In the last few years ago several methods such as physical, chemical, and biological used for the NPs synthesis. The physical methods for NPs synthesis such as pulse laser ablation, mechanical/ball milling, pulsed wire discharge,

* Corresponding author.
E-mail address: rohinitrivedi@mlsu.ac.in (R. Trivedi).

https://doi.org/10.1016/j.btre.2020.e00518

sputtering [35–39], etc. have been reported. The chemical synthesis includes colloidal [40,41], electrochemical [42,43], Chemical reduction [44], and photochemical [45] methods. The toxicity and relatively high material cost of these methods restricted their use in a better way. Biological method for NPs synthesis attracted researchers due to its simple, direct, non-toxicity, and ecofriendly characteristics upon chemical and physical methods. The biological method of NPs synthesis carried out by various sources bacterial, fungal, actinomycetes, yeast, algal, viruses [46–51], and plant extracts. Plants are reservoir of phytochemicals such as flavonoids, polyphenols, alkaloids, terpenoids, saponins, vitamins, polysaccharides, and proteins which act as reducing, capping and stabilizing agents for the biosynthesis of NPs [52]. *Celastrus paniculatus (C. paniculatus)* commonly known as black oil plant, Malkangani, and Jyotishmati is a traditional ayurvedic medicinal plant of family Celastraceae. The phytochemicals in crude extracts of *C. paniculatus* found alkaloids, flavonoids, phenylpropanoids, diterpenoids, triterpenoids, tetraterpenes, β-dihydroagarofuranoids, lignans, etc. [53].

This study reports a green route for the synthesis of CuNPs using *C. paniculatus* leaf extract, evaluation of its antifungal activity against phytopathogenic fungi *Fusarium oxysporum* (*F. oxysporum*), and its photocatalytic efficiency in the decomposition of organic dye. There is no report of *C. paniculatus* leaf extract mediated green synthesis of CuNPs and application in antifungal and photocatalytic activity to date.

2. Materials and methods

2.1. Materials

Copper (II) Sulfate pentahydrate ($CuSO_4.5H_2O$, CAS-No: 7758-99-8), was purchased from Sigma Aldrich. Methylene blue AR (RM116) was obtained from Himedia and *F. oxysporum* (ITCC No. 4998) procured from IAARI, New Delhi. The leaf samples of *C. paniculatus* were collected from Madan Mohan Malviya Government Ayurvedic College, Udaipur (Raj.) India. Collected plant material was authenticated by Herbarium, Botany Department, University of Rajasthan, Jaipur, India (No. RUBL211672). Deionized water was used to prepare plant extract and copper sulfate solution.

2.2. Methodology

2.2.1. Preparation of plant extract

Collected leaves were rinsed with tap water to remove dust particles. Further, leaves were rinsed with double distilled water (DDW) and shade dried for 1 week to remove the moisture content. The dried leaves were powdered in grinder mixer and powder stored in dark at ambient temperature. To prepare the plant extract, 2 gm of dried leaf powder was added in 200 mL deionized water in 500 mL flask, mixed well on a magnetic stirrer with hot plate at 60 °C for 20 min. The prepared extract was filtered using Whatman filter paper with size 11 μm followed by vacuum filtration using cellulose nitrate membrane. The filtrate was used immediately or stored at 4 °C for further use.

2.2.2. Synthesis of nanoparticles

For the synthesis of *C. paniculatus* copper nanoparticles, 50 mL (5 mM) copper sulfate solution was mixed with 5 mL of aqueous plant extract [54]. The pH value 7.0 adjusted for the mixture by the addition of NaOH (1 N) solution. Further, the green color mixture was obtained. The mixture centrifuged, pellets collected and dried overnight in a hot air oven at 60 °C. A dark green color powder obtained was stored at room temperature for further use.

2.2.3. Photocatalytic activity

The Photocatalytic activity of the CuNPs was evaluated by the degradation of MB in an aqueous solution under sunlight irradiation. Stock solution (10 mg/l) of MB was prepared. In the experiment, 10 mg CuNPs mixed with 100 mL of 10 mg/l MB solution and pH adjusted to 9.0 in the dark at ambient temperature [55]. Afterward, the resulting solution was kept under direct sunlight with a solar flux of 1100 lx measured by lux meter. About 3 mL aliquot of the suspension was taken and centrifuged at selected time intervals (every 15 min) to remove suspended CuNPs. The rate of dye degradation was determined by measuring the absorption spectrum using a UV–vis spectrophotometer at 664 nm. The photocatalytic degradation efficiency was assessed based on the formula.

$$\%\ \text{Degradation efficiency} = \frac{(C_0 - C)}{C_0} \times 100$$

Where, C_0 is the initial MB concentration, C is residual MB concentration after time t.

2.2.4. Antifungal activity

Antifungal activity of CuNPs was accessed using poison food technique against *F. oxysporum*. In this study, seven treatments (one control with water and three CuNPs at 0.12, 0.18 and 0.24 %, w/v in water along with 0.1 %, 1 % $CuSO_4$, and plant extract) were performed to evaluate antifungal activity. These treatments carried out in triplicate and the experiment was repeated thrice. The treated plated compared with control (without CuNPs) to calculate the % mycelial inhibition rate by using the formula given by Vincent [56].

$$(\%\ \text{Inhibition rate}) = \frac{(M_c - M_t)}{M_c} X\ 100$$

Where M_c is the mycelial growth in control, M_t is the mycelial growth in treatment.

3. Characterization of CuNPs

The absorbance spectrum of green synthesized CuNPs was analyzed using UV–vis spectroscopy (ELICO SL-159 UV–vis spectrophotometer) in the range of 220−540 nm. The morphological features of CuNPs were studied by using the transmission electron microscopy (TEM) (FEI Tecnai G2 20) and scanning electron microscopy (SEM). The elemental composition of the particles was examined by Energy-Dispersive X-ray spectroscopy (EDS) using JEOL SM-7600 F, Japan model. Fourier-transform infrared spectroscopy (FT-IR) analysis was employed to find out the role of biomolecules in leaf extract for metal reduction in the range of 500-4000 cm^{-1}. The charge and size distribution of CuNPs was measured using Malvern Zetasizer (Malvern Instrument Inc., London, U.K). Dynamic light scattering (DLS) measurements were performed by dispersing 20 mg CuNPs powder in 40 mL deionized water. The solution was stirred in a vortex mixer for 5 min to break up any aggregates and then 1−2 ml was transferred to the zeta-disposable cell.

4. Results and discussion

4.1. UV–vis spectra of CuNPs

Primarily, the formation of CuNPs confirmed by the change in color from yellow to green upon the addition of plant extract into aqueous $CuSO_4$ solution. The interaction between conduction electrons of metal NPs and incident photons was responsible for color change [57]. Further, CuNPs synthesis confirmed by a characteristic peak obtained at 269 nm (Fig. 1) [58,16]. In this

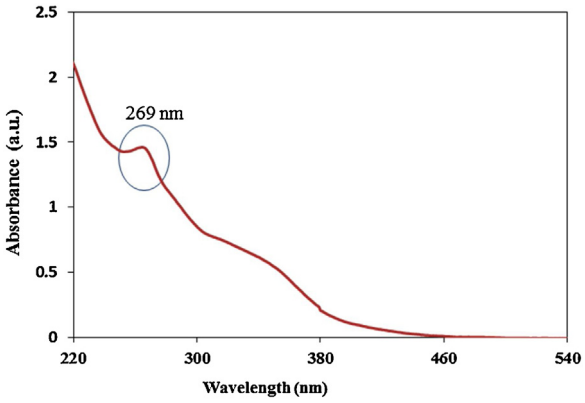

Fig. 1. UV–vis absorption spectrum.

experiment, effect of pH 7 on reduction of $CuSO_4$ into CuNPs was assessed by UV–vis spectroscopy. The neutral pH sharp absorbance peak was observed which may be due to the ionization of the phenolic groups present in plant extract [59]. The peak value was found to be gradually decreased with an increase in particle size (Fig. 1). This experiment concluded that the pH 7 is optimum for reduction of Cu^{2+} ions into CuNPs.

4.2. FT-IR characterization of CuNPs

FT-IR studies find out the possible biomolecules in plant extract which are responsible for the reduction and stabilization of CuNPs. FTIR spectra of *C. paniculatus* leaf extract have shown in Fig. 2, where the spectra of *C. paniculatus* leaf extract depicted broad peaks at 3315.28 cm^{-1} representing the hydroxyl (—OH) functional group in alcohols and phenolic compounds and 1635.50 cm^{-1} can be assigned to the aromatic bending of alkene group (C=C), while smaller peaks at 526.98–452.95 cm^{-1} are also assigned to the aromatic bending vibration of alkane groups (C—H) (Fig. 2). The FTIR spectrum of CuNPs depicts the distinctive characteristic bands at 3264.52 and 1636.62 cm^{-1} corresponds to the *C. paniculatus* leaf extract bands (Fig. 3). These peaks indicate the presence of flavonoid and other phenolic compounds in the plant leaf extract [60,61]. The flavonoid biomolecules transformed enol-form to the keto-form by releasing a reactive hydrogen atom and that can reduce Cu^{2+} ions to form CuNPs. These biomolecules stabilizes NPs by chelating with metal ions with their carbonyl groups or π-electrons [62]. Thus, results conclude that the surface of synthesized CuNPs was capped and stabilized by flavonoid and other phenolic compounds in the *C. paniculatus* leaf extract.

4.3. Morphological characterization of CuNPs

4.3.1. SEM, TEM and EDS analysis

The morphological characterization of CuNPs was carried out using SEM-EDS and TEM analyses. SEM analysis revealed the presence of spherical particles with some agglomeration due to sampling preparation (Fig. 4a-b). The size of the particles was calculated by the TEM and SEM analysis was found to be in the range of 2–10 nm with an average particle diameter of 5 nm as displayed in size distribution histogram (Fig. 5b).

The EDS analyses confirmed the composition and stability of synthesized CuNPs (Fig. 4c). The purity levels of the particles were examined, which indicated that *C. paniculatus* mediated CuNPs had 79.87 % of Cu and some weak signals of C, O, Si, S, Ca and Zn elements (Table 1). These weak signals may be due to the X-ray emission from the macromolecules like flavonoids, phenolic compounds, carbohydrates, glycosides, steroids and tannins present in the extracts [63].

4.4. Dynamic light scattering (DLS) studies

DLS analysis was used to find out the size and surface charge of NPs through the colloidal solutions. In the present study, the negative zeta potential was found at -22.2 mV and zeta deviation was 3.61 mV (Fig. 6a). The high negative value of zeta potential specifies a strong repellent force among the particles and prevents agglomeration [64,65]. The polydispersity index value of CuNPs was 1.000. Fig. 6b shows green synthesized CuNPs average particle size distribution was 290 nm. The larger size of CuNPs due to the measured size included biomolecule and water layer covering the surface of NPs [66]. It suggested that the size and charge

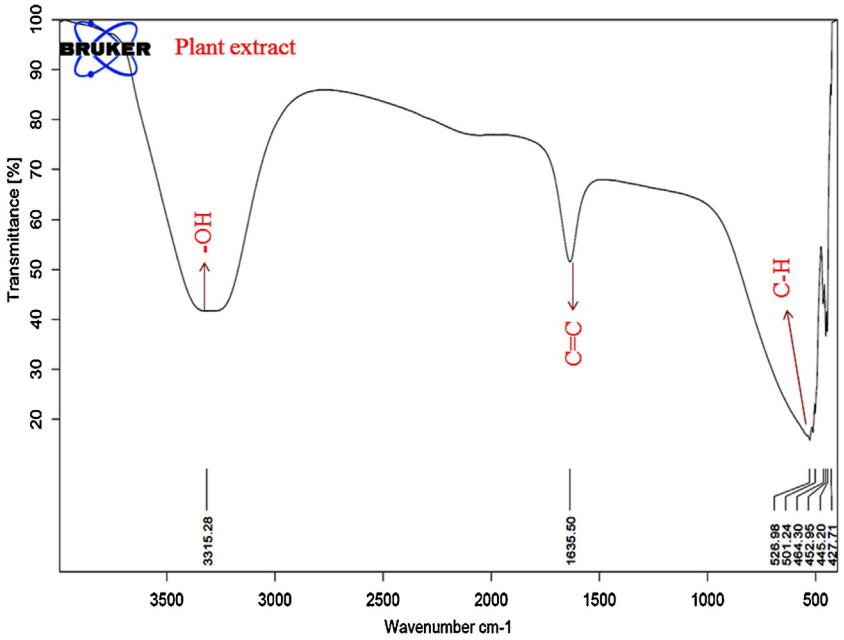

Fig. 2. FT-IR spectra of aqueous *C. paniculatus* leaves extract.

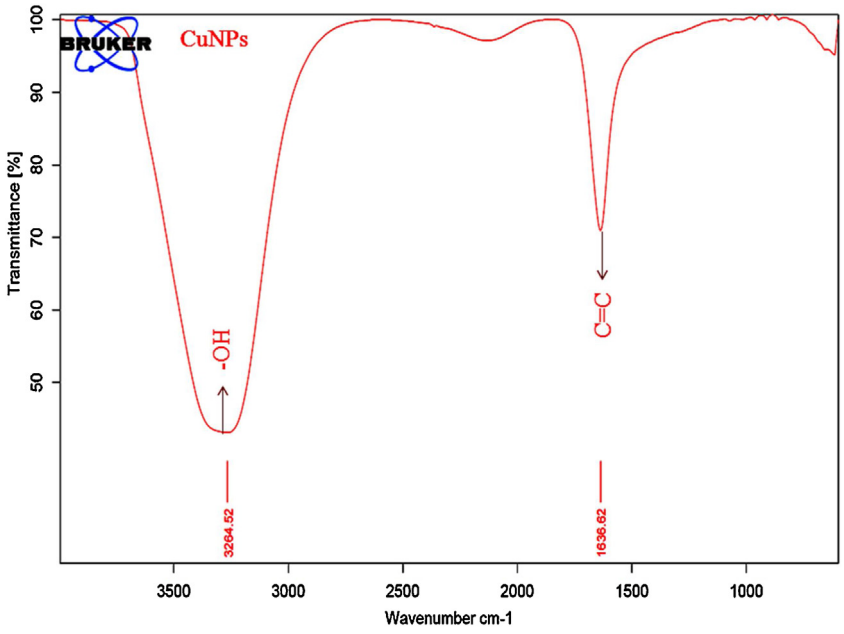

Fig. 3. FT-IR spectra of synthesized CuNPs.

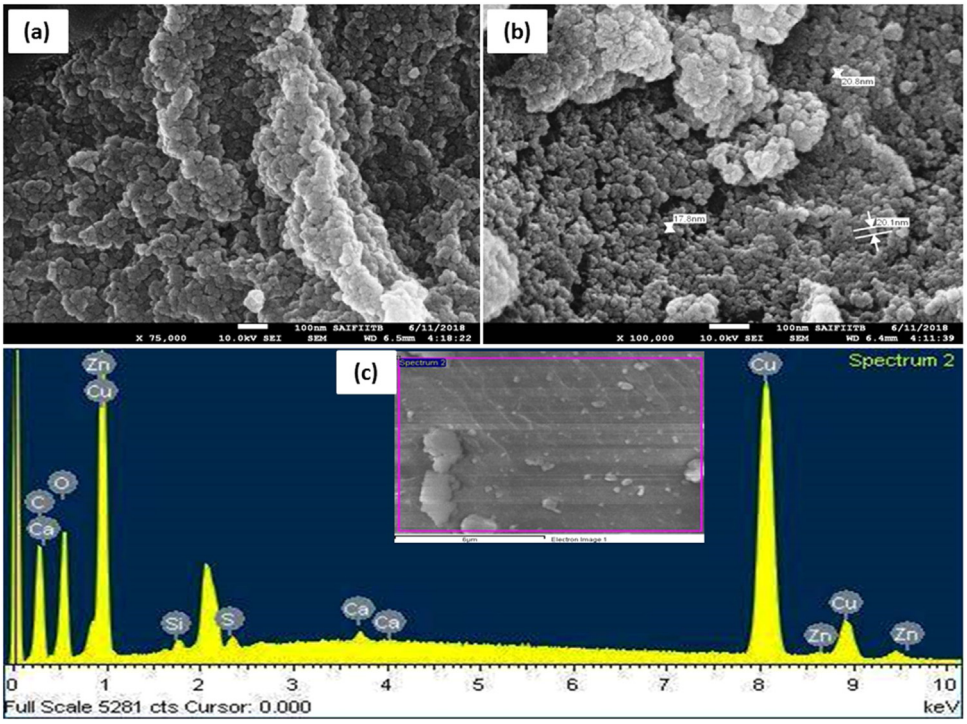

Fig. 4. (a-b) SEM micrographs of CuNPs, (c) EDS spectrum.

distribution of the synthesized NPs promoted or enhanced the biological property of CuNPs [67].

4.5. Photocatalytic degradation of MB

The potential of synthesized CuNPs for photocatalytic degradation of MB was examined under direct sunlight. The time dependent decrease in the absorption band intensity of MB dye was observed after the addition of CuNPs under solar light exposure. The photocatalytic degradation efficiency measured using spectrophotometer at 664 nm. In the experiment 10 mg L^{-1} concentration of MB mixed with 10 mg dosages of photocatalyst. Almost complete degradation of MB seen in 120 min (Fig. 7). In the presence of CuNPs the photodegradation was significantly enhanced at basic pH (pH = 9). The basic pH influences the surface charge properties of photocatalyst, the anionic dye molecule is negatively charged adsorbed on the photocatalyst surface [68]. The high pH favors adsorption of dye on the photocatalyst surface. The calculated degradation efficiency for MB was 90 % plotted in Fig. 8. The degradation experiments were performed with control (both in presence and absence of catalyst) were carried out in the dark to nullify any possibility of dye self-degradation, dye adsorption, and

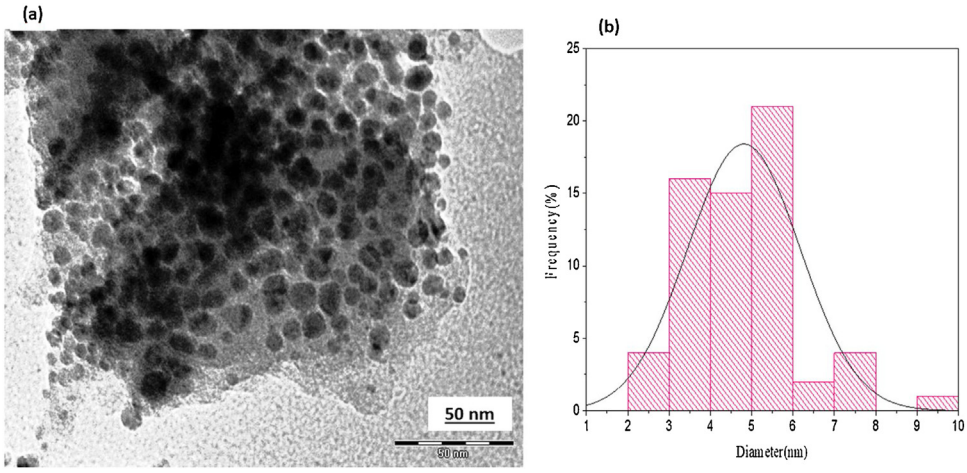

Fig. 5. (a) TEM micrograph of CuNPs, (b) Size distribution histogram of CuNPs.

Table 1
Compositional and particle stability analysis of CuNPs.

Element	Weight%	Atomic%
C K	13.02	39.92
O K	5.32	12.25
Si K	0.27	0.35
S K	0.40	0.46
Ca K	0.28	0.26
Cu K	79.87	46.29
Zn K	0.84	0.47
Totals	**100.00**	

catalytic activity of CuNPs in dark. Under dark conditions, CuNPs have not exhibited any insignificant effect on degradation of dye. Thus, experiments concluded that the dyes were not significantly degraded in dark conditions. Besides, dye degradation experiments performed under direct sunlight in the absence of catalyst showed negligible dye degradation while with catalyst dye almost completely degraded (Fig. 8). These experiments depicted that dye degradation was driven by a photocatalytic process.

In general, there were following steps in the photocatalytic degradation which is summarized below.

$$Cu + h\nu \rightarrow Cu\ (e^- + h^+) \quad \text{(i)}$$

Firstly, the CuNPs absorbed the solar irradiation get photo excited due to SPR influence (Eq. (ii)). Secondly, the electron and holes produced can react with O_2 (Eq. (iii)) and H_2O (Eq. (iv)) particles to provide active hydroxyl radical (OH^-), and anionic superoxide radical (O_2^-), respectively (Eq. (v)).

$$Cu + h\nu \rightarrow Cu\ (e^-) + Cu\ (h^+) \quad \text{(ii)}$$

$$Cu\ (e^-) + O_2 \rightarrow O_2^- \quad \text{(iii)}$$

$$Cu\ (h^+) + H_2O \rightarrow OH^- \quad \text{(iv)}$$

$$O_2^- \text{ or } OH^- + \text{Dye} \rightarrow \text{degraded product} \quad \text{(v)}$$

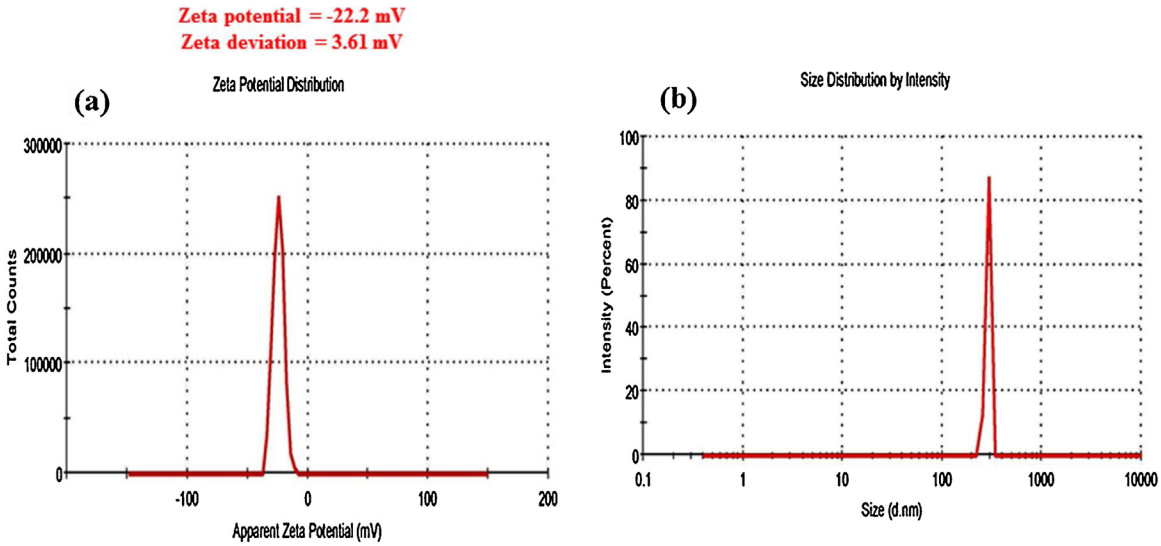

Fig. 6. DLS analysis of Cu NPs (a) zeta potential, (b) Size distribution.

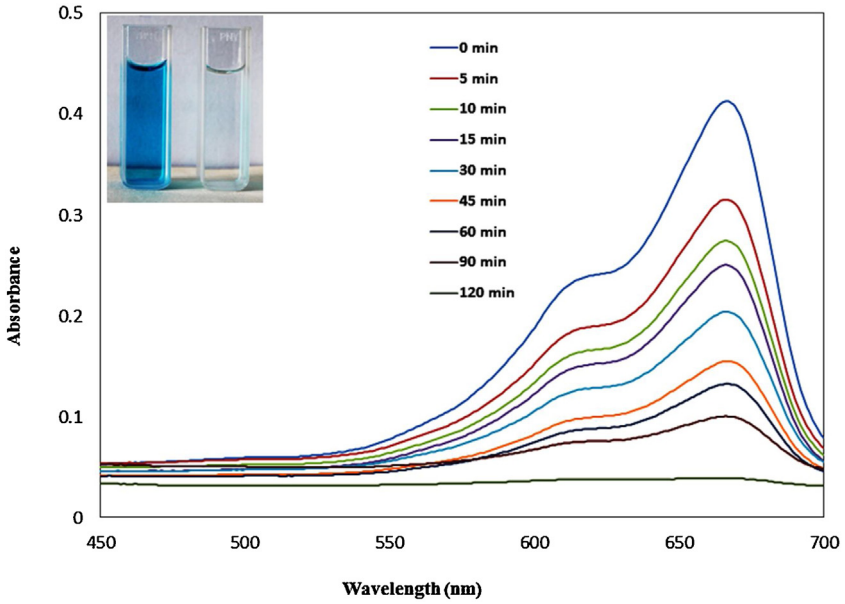

Fig. 7. Photocatalytic degradation of MB using CuNPs.

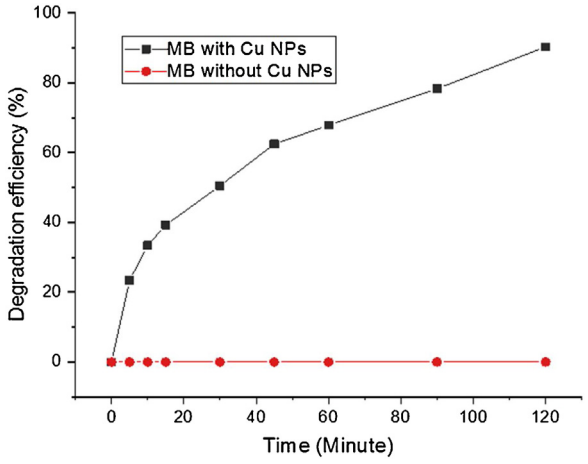

Fig. 8. Photocatalytic degradation efficiency of MB under sunlight irradiation.

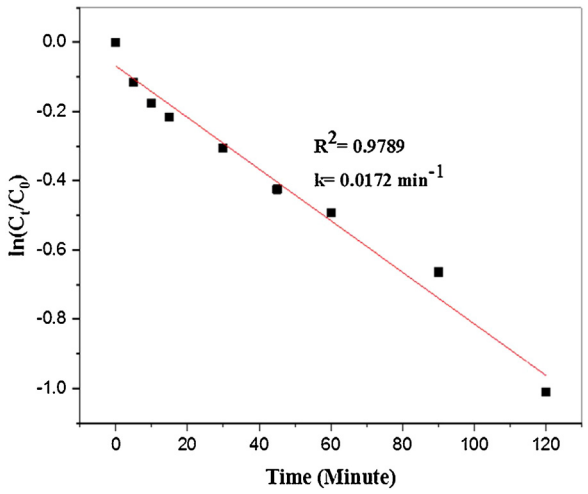

Fig. 9. Kinetic data for the degradation of aqueous MB under sunlight irradiation.

Finally, both oxidation as well as reduction proceeds on the photocatalyst surface. These highly reactive $^{\bullet}OH$ and $^{\bullet}O_2$ radicals can interface with the MB aromatic ring and possibly break the bond producing CO_2, H_2O, and numerous ions as by-products. The literature sharma and dutta [69] described that hydroxyl radical were dominant reactive oxygen species that contributed to degradation using NPs. Thus, their study provided the suitable justification for active species based photocatalytic degradation of dyes when using CuNPs, as discussed in our work.

The kinetics of the photocatalyzed decolorization process described by a pseudo first-order reaction for the concentration of MB [70].

$$\ln\frac{C_t}{C_0} = -K_t$$

Where, C_0 is the initial MB concentration and C_t is the MB concentration at the irradiation time (t) and k is the rate constant (min^{-1}). The linear relationship between $\ln(C_t/C_0)$ vs irradiation time (t) described in Fig. 9 showed good linear correlation with the values of correlation coefficient (R^2>95). The slope of the linear fitting line as shown in Fig. 9 concluded the rate constant (k) of the reaction was found 0.0172 min^{-1}. From this study we have concluded that the time duration for degradation of MB dye was 120 min. pseudo first-order kinetics resulted that obtained value of rate constant was found to be 0.0172 min-1. A comparative study of photocatalytic reduction of MB using different types of photocatalyst described in Table 2.

Table 2
Comparison of various photocatalysts in the reduction of MB.

S. No	Photocatalyst	Time	Ref.
	AuNPs	8 min	[71]
	AgNPs	45 min	[72]
	SnO_2 NPs	70 min	[73]
	rGO/TiO_2/Co_3O_4 NPs	120 min	[74]
	Sb-ZnO NPs	210 min	[75]
	CuNPs	120 min	This work

Degradation mechanism of MB

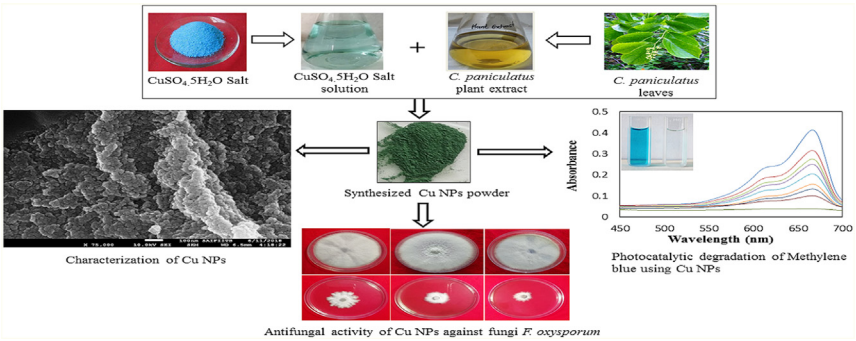

5. Antifungal assay of CuNPs

The antifungal activity of the synthesized CuNPs was assessed against *F. oxysporum* by measuring the mycelial radial growth. Study results showed that *F. oxysporum* exhibited mycelial growth inhibition at 0.24, 0.18, and 0.12 % CuNPs concentration (Fig. 10). CuNPs showed 76.29 ± 1.52, 73.70 ± 1.52 and 59.25 ± 0.57 mycelial growth inhibition at 0.24 and 0.18 and 0.12 %, respectively (Table 3). Maximum mycelial growth inhibition observed at 0.24 % CuNPs. The experiment, confirmed that mycelial growth inhibition depends on NPs concentrations. Commercial fungicide bavistin (0.1 %) was used as a positive control showing 100 % inhibition of fungal mycelial growth (Fig. 10). Whereas $CuSO_4$ (1.0 %) showed 20.74 ± 1.52 inhibition and plant extract was found ineffective in inhibiting mycelial growth and spore germination. Possible mechanisms of action of CuNPs are based on changes in the structure and function of fungi cell. Furthermore, these particles can affect macromolecule DNA, its replication and protein synthesis which ultimately lead to death of fungi. Similar studies have been reported for the antifungal activity of CuNPs against different fungi [76,77].

6. Conclusion

In the present study, CuNPs synthesized by a simple and benign method from leaf extract of *C. paniculatus*. The characterization studies revealed the morphological parameters and role of stabilizing agents during CuNPs synthesis. The TEM and SEM results concluded that the particles were spherical shaped and monodispersed with size ranging from 2 to 10 nm. The purity of green synthesized examined by EDS studies. The flavonoid and other phenolic compounds present in the *C. paniculatus* leaf extract reduce Cu^{2+} ions into CuNPs confirmed by FT-IR studies. The DLS studies revealed that biological property of CuNPs enhanced by the size and charge distribution of the NPs. The synthesized CuNPs exploited as photocatalyst exhibited excellent degradation efficiency on organic dye MB under

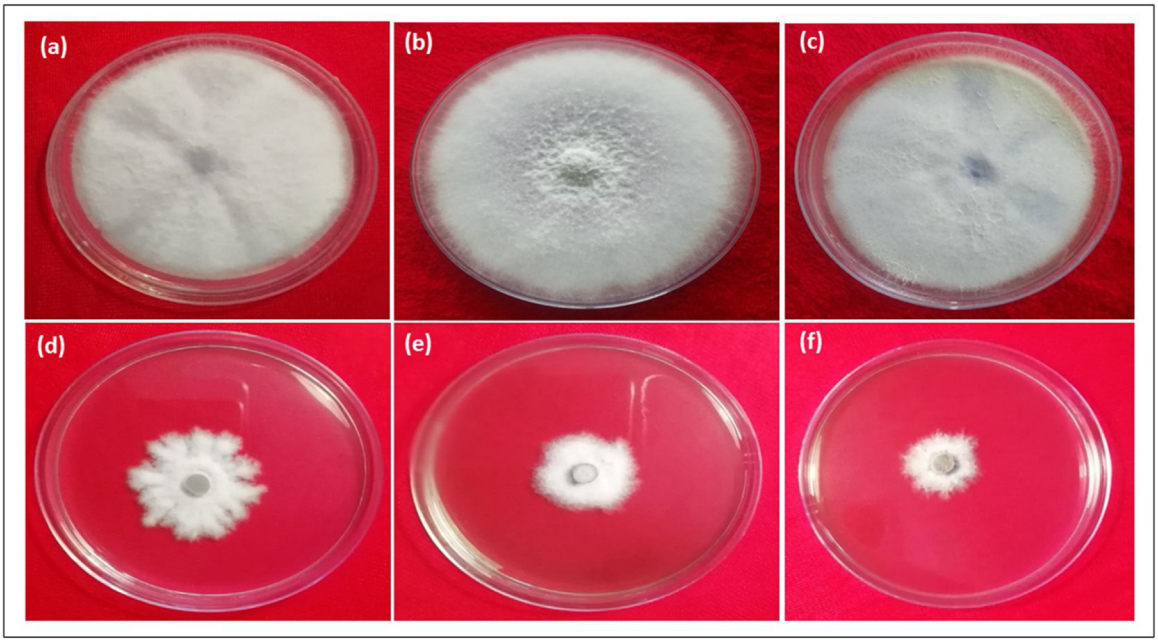

Fig. 10. Antifungal activity (a) control, (b) plant extract, (c) 1 % CuSO4, and CuNPs (d, e, f) 0.12, 0.18 and 0.24 % respectively.

Table 3
Effect of CuNPs on *in vitro* mycelial growth of *F. oxysporum*.

Treatment (%)	% Inhibition (mycelial growth) *F. oxysporum*
Control	0.0 ± 0.0
CuNPs	
0.12	59.25 ± 0.57
0.18	73.70 ± 1.52
0.24	76.29 ± 1.52
$CuSO_4$ (1%)	20.74 ± 1.52
Plant extract	0.0 ± 0.0
Bavistin (0.1 %)	100 ± 0.0

The mycelial growth inhibition of CuNP was performed in triplicate. Standard deviation values are given in the above mentioned table.

sunlight. The dye adsorption results were compared with previously reported literature. The synthesized CuNPs showed significant antifungal activity against *F. oxysporum* as demonstrated using the poison food technique. The overall study revealed that CuNPs successfully synthesized by green route and used as photocatalyst and antifungal agents.

Declaration of Competing Interest

The authors report no declarations of interest.

Acknowledgments

The author gratefully acknowledges DBT-JRF fellowship F. No. DBT/JRF/BET 16/I/2016/AL/63 New Delhi, India for financial support to Suresh Chand Mali. The authors also thank UGC-DAE, Indore for TEM, and IIT SAIF, Bombay for SEM-EDS Analysis.

Appendix A. Supplementary data

Supplementary material related to this article can be found, in the online version, at doi:https://doi.org/10.1016/j.btre.2020.e00518.

References

[1] K. Naseem, R. Begum, W. Wu, A. Irfan, A.G. Al-Sehemi, Z.H. Farooqi, Catalytic reduction of toxic dyes in the presence of silver nanoparticles impregnated core-shell composite microgels, J. Clean. Prod. 211 (2019) 855–864, doi:http://dx.doi.org/10.1016/j.jclepro.2018.11.164.
[2] S. Daniel, P.S. Syed, Shabudeen Sequestration of carcinogenic dye in waste water by utilizing an encapsulated activated carbon with nano MgO, Int. J. Chemtech Res. 7 (2014) 2235–2243.
[3] S. Vasantharaj, S. Sathiyavimal, M. Saravanan, P. Senthilkumar, K. Gnanasekaran, M. Shanmugavel, A. Pugazhendhi, Synthesis of ecofriendly copper oxide nanoparticles for fabrication over textile fabrics: characterization of antibacterial activity and dye degradation potential, J. Photochem. Photobiol. B Biol. 191 (2019) 143–149, doi:http://dx.doi.org/10.1016/j.jphotobiol.2018.12.026.
[4] A. Latif, S. Noor, Q.M. Sharif, M. Najeebullah, Different techniques recently used for the treatment of textile dyeing effluents: a review, J. Chem. Soc. Pak. 32 (2010) 115–116.
[5] K. Pakzad, H. Alinezhad, M. Nasrollahzadeh, Green synthesis of Ni@Fe3O4 and CuO nanoparticles using *Euphorbia maculata* extract as photocatalysts for the degradation of organic pollutants under UV-irradiation, Ceram. Int. 45 (2019) 17173–17182, doi:http://dx.doi.org/10.1016/j.ceramint.2019.05.272.
[6] Z. Issaabadi, M. Nasrollahzadeh, S.M. Sajadi, Green synthesis of the copper nanoparticles supported on bentonite and investigation of its catalytic activity, J. Clean. Prod. 142 (2017) 3584–3591, doi:http://dx.doi.org/10.1016/j.jclepro.2016.10.109.
[7] Y.A. Selim, M.A. Azb, I. Ragab, M.H.M. Abd El-Azim, Green synthesis of zinc oxide nanoparticles using aqueous extract of *Deverra tortuosa* and their cytotoxic activities, Sci. Rep. 10 (2020) 1–9, doi:http://dx.doi.org/10.1038/s41598-020-60541-1.
[8] P.A. Luque, O. Nava, C.A. Soto-Robles, A.R. Vilchis-Nestor, H.E. Garrafa-Galvez, A. Castro Beltran, Effects of *Daucus carota* extract used in green synthesis of zinc oxide nanoparticles, J. Mater. Sci. Mater. Electron. 29 (2018) 17638–17643, doi:http://dx.doi.org/10.1007/s10854-018-9867-5.
[9] P.V. Kumar, S.M. Jelastin Kala, K.S. Prakash, Green synthesis derived Pt-nanoparticles using *Xanthium strumarium* leaf extract and their biological studies, J. Environ. Chem. Eng. 7 (2019) 103146, doi:http://dx.doi.org/10.1016/j.jece.2019.103146.
[10] A.A. Olajire, A.A. Mohammed, Green synthesis of palladium nanoparticles using *Ananas comosus* leaf extract for solid-phase photocatalytic degradation of low density polyethylene film, J. Environ. Chem. Eng. 7 (2019) 103270, doi:http://dx.doi.org/10.1016/j.jece.2019.103270.
[11] B. Khodadadi, M. Bordbar, M. Nasrollahzadeh, *Achillea millefolium* L. extract mediated green synthesis of waste peach kernel shell supported silver nanoparticles: application of the nanoparticles for catalytic reduction of a variety of dyes in water, J. Colloid Interface Sci. 493 (2017) 85–93, doi:http://dx.doi.org/10.1016/j.jcis.2017.01.012.
[12] M. Behravan, A.H. Panahi, A. Naghizadeh, M. Ziaee, R. Mahdavi, A. Mirzapour, Facile green synthesis of silver nanoparticles using *Berberis vulgaris* leaf and root aqueous extract and its antibacterial activity, Int. J. Biol. Macromol. 124 (2019) 148–154, doi:http://dx.doi.org/10.1016/j.ijbiomac.2018.11.101.
[13] I. Bibi, N. Nazar, M. Iqbal, S. Kamal, H. Nawaz, S. Nouren, F. Rehman, Green and eco-friendly synthesis of cobalt-oxide nanoparticle: characterization and photo-catalytic activity, Adv. Powder Technol. 28 (2017) 2035–2043, doi:http://dx.doi.org/10.1016/j.apt.2017.05.008.
[14] S.M. Sajadi, M. Nasrollahzadeh, M. Maham, Aqueous extract from seeds of *Silybum marianum* L. as a green material for preparation of the Cu/Fe3O4 nanoparticles: a magnetically recoverable and reusable catalyst for the reduction of nitroarenes, J. Colloid Interface Sci. 469 (2016) 93–98, doi:http://dx.doi.org/10.1016/j.jcis.2016.02.009.
[15] M. Nasrollahzadeh, S.M. Sajadi, Preparation of Au nanoparticles by *Anthemis xylopoda* flowers aqueous extract and their application for alkyne/aldehyde/amine A3-type coupling reactions, RSC Adv. 5 (2015) 46240–46246, doi:http://dx.doi.org/10.1039/c5ra08927a.
[16] S. Chand Mali, S. Raj, R. Trivedi, Biosynthesis of copper oxide nanoparticles using *Enicostemma axillare* (Lam.) leaf extract, Biochem. Biophys. Rep. 20 (2019) 100699, doi:http://dx.doi.org/10.1016/j.bbrep.2019.100699.
[17] S. Rajeshkumar, S. Menon, S.V. Kumar, M.M. Tambuwala, H.A. Bakshi, M. Mehta, K. Dua, Antibacterial and antioxidant potential of biosynthesized copper nanoparticles mediated through *Cissus arnotiana* plant extract, J. Photochem. Photobiol. B Biol. 197 (2019) 111531, doi:http://dx.doi.org/10.1016/j.jphotobiol.2019.111531.
[18] M. Bordbar, N. Negahdar, M. Nasrollahzadeh, *Melissa Officinalis* L. leaf extract assisted green synthesis of CuO/ZnO nanocomposite for the reduction of 4-nitrophenol and Rhodamine B, Sep. Purif. Technol. 191 (2018) 295–300, doi:http://dx.doi.org/10.1016/j.seppur.2017.09.044.
[19] M. Nasrollahzadeh, M. Sajjadi, S. Mohammad Sajadi, Biosynthesis of copper nanoparticles supported on manganese dioxide nanoparticles using *Centella asiatica* L. leaf extract for the efficient catalytic reduction of organic dyes and nitroarenes Cuihua Xuebao/Chinese, J. Catal. 39 (2018) 109–117, doi:http://dx.doi.org/10.1016/S1872-2067(17)62915-2.
[20] N. Nagar, V. Devra, Green synthesis and characterization of copper nanoparticles using *Azadirachta indica* leaves, Mater. Chem. Phys. 213 (2018) 44–51, doi:http://dx.doi.org/10.1016/j.matchemphys.2018.04.007.
[21] M. Nasrollahzadeh, S. Mohammad Sajadi, A. Rostami-Vartooni, Green synthesis of CuO nanoparticles by aqueous extract of *Anthemis nobilis* flowers and their catalytic activity for the A3 coupling reaction, J. Colloid Interface Sci. 459 (2015) 183–188, doi:http://dx.doi.org/10.1016/j.jcis.2015.08.020.
[22] H.J. Lee, J.Y. Song, B.S. Kim, Biological synthesis of copper nanoparticles using *Magnolia kobus* leaf extract and their antibacterial activity, J. Chem. Technol. Biotechnol. 88 (2013) 1971–1977, doi:http://dx.doi.org/10.1002/jctb.4052.
[23] M. Hafeez, R. Arshad, J. Khan, B. Akram, M.N. Ahmad, M.U. Hameed, S. Haq, *Populus ciliata* mediated synthesis of copper oxide nanoparticles for potential biological applications, Mater. Res. Express 6 (2019) 055043, doi:http://dx.doi.org/10.1088/2053-1591/ab0601.
[24] E.V.R. Campos, P.L.F. Proença, J.L. Oliveira, M. Bakshi, P.C. Abhilash, L.F. Fraceto, Use of botanical insecticides for sustainable agriculture: future perspectives, Ecol. Indic. 105 (2019) 483–495, doi:http://dx.doi.org/10.1016/j.ecolind.2018.04.038.
[25] J.R. Lamichhane, E. Osdaghi, F. Behlau, J. Köhl, J.B. Jones, J.N. Aubertot, Thirteen decades of antimicrobial copper compounds applied in agriculture. A review, Agron. Sustain. Dev. 38 (2018) 28, doi:http://dx.doi.org/10.1007/s13593-018-0503-9.
[26] B. Rashid, T. Husnain, S. Riazuddin, Herbicides and pesticides as potential pollutants: a global problem in Plant, Adapt. Phytorem. (2010) 427–447.
[27] J.R. Rohr, P.W. Crumrine, Effects of an herbicide and an insecticide on pond community structure and processes, Ecol. Appl. 15 (2005) 1135–1147, doi:http://dx.doi.org/10.1890/03-5353.
[28] A. Joshi, A. Sharma, R.K. Bachheti, A. Husen, V.K. Mishra, Plant-Mediated Synthesis of Copper Oxide Nanoparticles and Their Biological Applications in Nanomaterials and Plant Potential, (2019) , pp. 221–237.
[29] P. Kalatehjari, M. Yousefian, M.A. Khalilzadeh, Assessment of antifungal effects of copper nanoparticles on the growth of the fungus *Saprolegnia* sp. on white fish (*Rutilus frisii kutum*) eggs Egypt, Int. J. Aquat. Res. 41 (2015) 303–306, doi:http://dx.doi.org/10.1016/j.ejar.2015.07.004.
[30] R. Katwal, H. Kaur, G. Sharma, M. Naushad, D. Pathania, Electrochemical synthesized copper oxide nanoparticles for enhanced photocatalytic and antimicrobial activity, J. Ind. Eng. Chem. 31 (2015) 173–184, doi:http://dx.doi.org/10.1016/j.jiec.2015.06.021.
[31] A. Kumar, G. Sharma, M. Naushad, P. Singh, S. Kalia, Polyacrylamide/Ni0.02Zn0.98O nanocomposite with high solar light photocatalytic activity and efficient adsorption capacity for toxic dye removal, Ind. Eng. Chem. Res. 53 (2014) 15549–15560, doi:http://dx.doi.org/10.1021/ie5018173.

[32] A. Yabuki, N. Arriffin, Electrical conductivity AR of copper nanoparticle thin films annealed at low temperature, Thin Solid Films 518 (2010) 7033–7037, doi:http://dx.doi.org/10.1016/j.tsf.2010.07.023.

[33] T.M.D. Dang, T.T.T. Le, E. Fribourg-Blanc, M.C. Dang, Synthesis and optical properties of copper nanoparticles prepared by a chemical reduction method, Adv. Nat. Sci. Nanosci. Nanotechnol. 2 (2011) 015009, doi:http://dx.doi.org/10.1088/2043-6262/2/1/015009.

[34] Q. Lv, B. Zhang, X. Xing, Y. Zhao, R. Cai, W. Wang, Q. Gu, Biosynthesis of copper nanoparticles using*Shewanella loihica* PV-4 with antibacterial activity: Novel approach and mechanisms investigation, J. Hazard. Mater. 347 (2018) 141–149, doi:http://dx.doi.org/10.1016/j.jhazmat.2017.12.070.

[35] M. Fernández-Arias, M. Boutinguiza, J. Del Val, C. Covarrubias, F. Bastias, L. Gómez, M. Maureira, F. Arias-González, A. Riveiro, J. Pou, Copper nanoparticles obtained by laser ablation in liquids as bactericidal agent for dental applications, Appl. Surf. Sci. 507 (2020) 145032, doi:http://dx.doi.org/10.1016/j.apsusc.2019.145032.

[36] T. Han, J. Li, N. Zhao, C. He, Microstructure and properties of copper coated graphene nanoplates reinforced Al matrix composites developed by low temperature ball milling, Carbon N. Y. 159 (2020) 311–323, doi:http://dx.doi.org/10.1016/j.carbon.2019.12.029.

[37] A. Abu-Oqail, A. Wagih, A. Fathy, O. Elkady, A.M. Kabeel, Effect of high energy ball milling on strengthening of Cu-ZrO2 nanocomposites, Ceram. Int. 45 (2019) 5866–5875, doi:http://dx.doi.org/10.1016/j.ceramint.2018.12.053.

[38] K. Sugashima, K. Suzuki, T. Suzuki, T. Nakayama, H. Suematsu, K. Niihara, Synthesis of zirconium carbide nanosized powders by pursed wire discharge in oleic acid, J. Korean Phys. Soc. 68 (2016) 345–350, doi:http://dx.doi.org/10.3938/jkps.68.345.

[39] M. Verma, I. Tyagi, R. Chandra, V.K. Gupta, Adsorptive removal of Pb (II) ions from aqueous solution using CuO nanoparticles synthesized by sputtering method, J. Mol. Liq. 225 (2017) 936–944, doi:http://dx.doi.org/10.1016/j.molliq.2016.04.045.

[40] P. Destro, Synthesis of Gold-copper Nanoparticles by Colloidal Method Varying the Compositions As a Function of the Synthesis Final Temperature in Colloidal Nanoparticles for Heterogeneous Catalysis, (2019) , pp. 17–40.

[41] I.A. Sabbah, M.F. Zaky, M.E. Hendawy, N.A. Negm, Synthesis, characterization and antimicrobial activity of colloidal copper nanoparticles stabilized by cationic thiol polyurethane surfactants, J. Polym. Res. 25 (2018) 252, doi:http://dx.doi.org/10.1007/s10965-018-1649-5.

[42] S. Das, V.C. Srivastava, Synthesis and characterization of ZnO/CuO nanocomposite by electrochemical method, Mater. Sci. Semicond. Process. 57 (2017) 173–177, doi:http://dx.doi.org/10.1016/j.mssp.2016.10.031.

[43] N. Dighore, S. Jadhav, S. Gaikwad, A. Rajbhoj, Copper oxide nanoparticles synthesis by electrochemical method Medziagotyra, Biomater. Sci. 22 (2016) 170–173, doi:http://dx.doi.org/10.5755/j01.ms.22.2.7501.

[44] P. Van Viet, H.T. Nguyen, T.M. Cao, L. Van Hieu, *Fusarium* antifungal activities of copper nanoparticles synthesized by a chemical reduction method, J. Nanomater. 2016 (2016), doi:http://dx.doi.org/10.1155/2016/1957612.

[45] M.B. Pori, B. Likozar, M. Marinšek, Z. Crnjak, Orel Preparation of Cu/ZnO-based heterogeneous catalysts by photochemical deposition, their characterisation and application for methanol synthesis from carbon dioxide and hydrogen, Fuel Process. Technol. 146 (2016) 39–47, doi:http://dx.doi.org/10.1016/j.fuproc.2016.02.021.

[46] P. Prema, P.A. Iniya, G. Immanuel, Microbial mediated synthesis, characterization, antibacterial and synergistic effect of gold nanoparticles using *Klebsiella pneumoniae* (MTCC-4030), RSC Adv. 6 (2016) 4601–4607, doi:http://dx.doi.org/10.1039/c5ra23982f.

[47] A.I. El-Batal, G.S. El-Sayyad, F.M. Mosallam, R.M. Fathy, *Penicillium chrysogenum*-mediated mycogenic synthesis of copper oxide nanoparticles using gamma rays for in vitro antimicrobial activity against some plant pathogens, J. Clust. Sci. 31 (2020) 79–90, doi:http://dx.doi.org/10.1007/s10876-019-01619-3.

[48] S.E.D. Hassan, A. Fouda, A.A. Radwan, S.S. Salem, M.G. Barghoth, M.A. Awad, A. M. Abdo, M.S. El-Gamal, Endophytic actinomycetes *Streptomyces* spp mediated biosynthesis of copper oxide nanoparticles as a promising tool for biotechnological applications, J. Biol. Inorg. Chem. 24 (2019) 377–393, doi:http://dx.doi.org/10.1007/s00775-019-01654-5.

[49] A. Sivaraj, V. Kumar, R. Sunder, K. Parthasarathy, G. Kasivelu, Commercial yeast extracts mediated green synthesis of silver chloride nanoparticles and their anti-mycobacterial activity, J. Clust. Sci. 31 (2020) 287–291, doi:http://dx.doi.org/10.1007/s10876-019-01626-4.

[50] A. Rahman, S. Kumar, T. Nawaz, Biosynthesis of Nanomaterials Using Algae in Microalgae Cultivation for Biofuels Production, (2020) , pp. 265–279.

[51] A.M. Wen, N.F. Steinmetz, Design of virus-based nanomaterials for medicine, biotechnology, and energy, Chem. Soc. Rev. 45 (2016) 4074–4126, doi:http://dx.doi.org/10.1039/c5cs00287g.

[52] A. Pugazhendhi, R. Prabhu, K. Muruganantham, R. Shanmuganathan, S. Natarajan, Anticancer, antimicrobial and photocatalytic activities of green synthesized magnesium oxide nanoparticles (MgONPs) using aqueous extract of *Sargassum wightii*, J. Photochem. Photobiol. B Biol. 190 (2019) 86–97, doi:http://dx.doi.org/10.1016/j.jphotobiol.2018.11.014.

[53] Y. Shen, B. lian Chen, Q. xiu Zhang, Y. zhong Zheng, Q. Fu, Traditional uses, secondary metabolites, and pharmacology of *Celastrus* species-a review, J. Ethnopharmacol. 241 (2019) 111934, doi:http://dx.doi.org/10.1016/j.jep.2019.111934.

[54] R. Sankar, P. Manikandan, V. Malarvizhi, T. Fathima, K.S. Shivashangari, V. Ravikumar, Green synthesis of colloidal copper oxide nanoparticles using *Carica papaya* and its application in photocatalytic dye degradation, Spectrochim. Acta - Part A Mol. Biomol. Spectrosc. 121 (2014) 746–750, doi:http://dx.doi.org/10.1016/j.saa.2013.12.020.

[55] T. Sinha, M. Ahmaruzzaman, Green synthesis of copper nanoparticles for the efficient removal (degradation) of dye from aqueous phase, Environ. Sci. Pollut. Res. 22 (2015) 20092–20100, doi:http://dx.doi.org/10.1007/s11356-015-5223-y.

[56] J.M. Vincent, Distortion of fungal hyphæ in the presence of certain inhibitors, Nature 159 (1947) 850, doi:http://dx.doi.org/10.1038/159850b0.

[57] J. Jana, M. Ganguly, T. Pal, Enlightening surface plasmon resonance effect of metal nanoparticles for practical spectroscopic application, RSC Adv. 6 (2016) 86174–86211, doi:http://dx.doi.org/10.1039/c6ra14173k.

[58] B. Turakhia, M.B. Divakara, M.S. Santosh, S. Shah, Green synthesis of copper oxide nanoparticles: a promising approach in the development of antibacterial textiles, J. Coat. Technol. Res. 17 (2020) 531–540, doi:http://dx.doi.org/10.1007/s11998-019-00303-5.

[59] G.A. Martínez-Castañón, N. Niño-Martínez, F. Martínez-Gutierrez, J.R. Martínez-Mendoza, F. Ruiz, Synthesis and antibacterial activity of silver nanoparticles with different sizes, J. Nanopart. Res. 10 (2008) 1343–1348, doi:http://dx.doi.org/10.1007/s11051-008-9428-6.

[60] O. Długosz, J. Chwastowski, M. Banach, Hawthorn berries extract for the green synthesis of copper and silver nanoparticles, Chem. Pap. 74 (2020) 239–252, doi:http://dx.doi.org/10.1007/s11696-019-00873-z.

[61] M.F. Al-Hakkani, Biogenic copper nanoparticles and their applications: a review, SN Appl. Sci. 2 (2020) 1–20, doi:http://dx.doi.org/10.1007/s42452-020-2279-1.

[62] A. Akturk, F.K. Güler, M.E. Taygun, G. Goller, S. Küçükbayrak, Synthesis and antifungal activity of soluble starch and sodium alginate capped copper nanoparticles, Mater. Res. Express 6 (2019) 1250g3, doi:http://dx.doi.org/10.1088/2053-1591/ab677e.

[63] H. Zhang, X. Lv, Y. Li, Y. Wang, J. Li, P25-graphene composite as a high performance photocatalyst, ACS Nano 4 (2010) 380–386, doi:http://dx.doi.org/10.1021/nn901221k.

[64] L. Lin, P. Qiu, X. Cao, L. Jin, Colloidal silver nanoparticles modified electrode and its application to the electroanalysis of Cytochrome c, Electrochim. Acta 53 (2008) 5368–5372, doi:http://dx.doi.org/10.1016/j.electacta.2008.02.080.

[65] R. Sankar, A. Karthik, A. Prabu, S. Karthik, K.S. Shivashangari, V. Ravikumar, *Origanum vulgare* mediated biosynthesis of silver nanoparticles for its antibacterial and anticancer activity, Colloids Surf. B Biointerfaces 108 (2013) 80–84, doi:http://dx.doi.org/10.1016/j.colsurfb.2013.02.033.

[66] S. Bhakya, S. Muthukrishnan, M. Sukumaran, M. Muthukumar, Biogenic synthesis of silver nanoparticles and their antioxidant and antibacterial activity, Appl. Nanosci. 6 (2016) 755–766, doi:http://dx.doi.org/10.1007/s13204-015-0473-z.

[67] R. Sankar, R. Maheswari, S. Karthik, K.S. Shivashangari, V. Ravikumar, Anticancer activity of *Ficus religiosa* engineered copper oxide nanoparticles, Mater. Sci. Eng. C 44 (2014) 234–239, doi:http://dx.doi.org/10.1016/j.msec.2014.08.030.

[68] A.F. Alkaim, A.M. Aljeboree, N.A. Alrazaq, S.J. Baqir, F.H. Hussein, A.J. Lilo, Effect of pH on adsorption and photocatalytic degradation efficiency of different catalysts on removal of methylene blue, Asian J. Chem. 26 (2014) 8445, doi:http://dx.doi.org/10.14233/ajchem.2014.17908.

[69] A. Sharma, R.K. Dutta, Studies on the drastic improvement of photocatalytic degradation of acid orange-74 dye by TPPO capped CuO nanoparticles in tandem with suitable electron capturing agents, RSC Adv. 5 (2015) 43815–43823, doi:http://dx.doi.org/10.1039/c5ra04179a.

[70] R. Singh, S. Dutta, Synthesis and characterization of solar photoactive TiO2 nanoparticles with enhanced structural and optical properties, Adv. Powder Technol. 29 (2018) 211–219, doi:http://dx.doi.org/10.1016/j.apt.2017.11.005.

[71] B. Paul, B. Bhuyan, D. Dhar Purkayastha, M. Dey, S.S. Dhar, Green synthesis of gold nanoparticles using *Pogestemon benghalensis* (B) O. Ktz. Leaf extract and studies of their photocatalytic activity in degradation of methylene blue, Mater. Lett. 148 (2015) 37–40, doi:http://dx.doi.org/10.1016/j.matlet.2015.02.054.

[72] V. Cittrarasu, B. Balasubramanian, D. Kaliannan, S. Park, V. Maluventhan, T. Kaul, W.C. Liu, M. Arumugam, Biological mediated Ag nanoparticles from *Barleria longiflora* for antimicrobial activity and photocatalytic degradation using methylene blue Artif. Cells, Nanomedicine Biotechnol. 47 (2019) 2424–2430, doi:http://dx.doi.org/10.1080/21691401.2019.1626407.

[73] G. Elango, S.M. Roopan, Efficacy of SnO_2 nanoparticles toward photocatalytic degradation of methylene blue Dye, J. Photochem. Photobiol. B Biol. 155 (2016) 34–38, doi:http://dx.doi.org/10.1016/j.jphotobiol.2015.12.010.

[74] R. Ranjith, V. Renganathan, S.M. Chen, N.S. Selvan, P.S. Rajam, Green synthesis of reduced graphene oxide supported TiO_2/Co_3O_4 nanocomposite for photocatalytic degradation of methylene blue and crystal violet, Ceram. Int. 45 (2019) 12926–12933, doi:http://dx.doi.org/10.1016/j.ceramint.2019.03.219.

[75] L. Chen, I. Batjikh, J. Hurh, Y. Han, Y. Huo, H. Ali, J.F. Li, E.J. Rupa, J.C. Ahn, R. Mathiyalagan, D.C. Yang, Green synthesis of zinc oxide nanoparticles from root extract of *Scutellaria baicalensis* and its photocatalytic degradation activity using methylene blue, Optik (Stuttg) 184 (2019) 324–329, doi:http://dx.doi.org/10.1016/j.ijleo.2019.03.051.

[76] E.Z. Gomaa, M.M. Housseiny, A.A.A.K. Omran, Fungicidal efficiency of silver and copper nanoparticles produced by *Pseudomonas fluorescens* ATCC 17397 against four *Aspergillus* species: a molecular study, J. Clust. Sci. 30 (2019) 181–196, doi:http://dx.doi.org/10.1007/s10876-018-1474-3.

[77] N. Pariona, A.I. Mtz-Enriquez, D. Sánchez-Rangel, G. Carrión, F. Paraguay-Delgado, G. Rosas-Saito, Green-synthesized copper nanoparticles as a potential antifungal against plant pathogens, RSC Adv. 9 (2019) 18835–18843, doi:http://dx.doi.org/10.1039/c9ra03110c.